THE AMERICAN SOCIETY OF MECHANICAL ENGINEERS
345 E. 47th St., New York, N.Y. 10017

97-GT-149

BREAK

SOOT MODELING IN GAS TURBINE COMBUSTORS

Anil K. Tolpadi
General Electric Research & Development Center
P.O. Box 8, MS K1–ES 206
Schenectady, NY 12301, USA

Allen M. Danis & Hukam C. Mongia
General Electric Aircraft Engines
Mail Drop E404
Cincinnati, OH 45215, USA

R. Peter Lindstedt
Department of Mechanical Engineering
Imperial College
London SW7 2BX, UK

ABSTRACT

A method is presented for predicting soot in gas turbine combustors. A soot formation/oxidation model due to Fairweather et al [1992] has been employed. This model has been implemented in the CONCERT code which is a fully elliptic three–dimensional (3–D) body–fitted computational fluid dynamics (CFD) code based on pressure correction techniques. The combustion model used here is based on an assumed probability density function (PDF) parameterized by the mean and variance of the mixture fraction and a β–PDF shape. In the soot modeling, two additional transport equations corresponding to the soot mass fraction and the soot number density are solved. As an initial validation, calculations were performed in a simple propane jet diffusion flame for which experimental soot concentration measurements along the centerline and along the radius at various axial downstream stations were available from the literature. Soot predictions were compared with measured data which showed reasonable agreement. Next, soot predictions were made in a 3–D model of a CF6–80LEC engine single annular combustor over a range of operating pressures and temperatures. Although the fuel in the combustor is Jet–A, the soot computations assumed propane to be the surrogate fuel. To account for this fuel change, the soot production term was increased by a factor of 10X. In addition, the oxidation term was increased by a factor of 4X to account for uncertainties in the assumed collision frequencies. The soot model was also tested against two other combustors, a CF6–80C and a CFM56–5B. Comparison of the predicted soot concentrations with measured smoke numbers showed fairly good correlation within the range of the soot model parameters studied. More work has to be performed to address several modeling issues including sensitivity to oxidation rate coefficients and scalar diffusion.

NOMENCLATURE

C_1, C_2, C_3 etc.	Soot model coefficients (defined on page 3)
C_a	Agglomeration rate constant (9.0)
C_{av}	Average combustor exit soot concentration
C_{min}	Number of Carbon atoms in incipent Carbon particle (100)
d	Fuel jet diameter (propane diffusion flame)
k	Boltzmann constant
M_{cs}	Molecular weight of Carbon (12.011)
N	Local soot particle number density (particles per unit mass)
N_A	Avogadro number
P3	Average combustor inlet pressure
SAE	SAE Smoke Number
T	Local fluid temperature
T3	Average combustor inlet temperature
x	Axial distance downstream from jet (propane diffusion flame)
Y_{cs}	Local soot mass fraction
ϱ	Local fluid density
ϱ_{cs}	Density of solid carbon (2000 kg/m^3)
[k]	Molar concentration for specie 'k' (kmol/m^3)

Presented at the International Gas Turbine & Aeroengine Congress & Exhibition
Orlando, Florida — June 2–June 5, 1997

INTRODUCTION

In a gas turbine combustor, there exists a wide range of complex, interacting physical and chemical phenomena. Some of these phenomena include (1) soot formation; (2)particulate behavior; (3)radiation; (4)finite−rate chemistry effects, notably for NO_x and CO emissions; (5)turbulent transport and (3)two−phase flow. Depending on the specific issues being addressed, models of varying degrees of sophistication have been employed. The level of sophistication in design models has continually increased over the years with improvements in numerical methods, computer capabilities, and physical understanding. In recent years, aircraft combustors are operating at higher fuel−air ratios in the primary zone thus making soot emissions from the engine an element of great concern. It is therefore important to have an ability to predict combustor soot levels. The development of a reliable smoke prediction model for aircraft engine combustors is extremely challenging due to the fact that the final soot levels measured in the exhaust of these combustors are orders of magnitude smaller than that measured in laboratory flames.

In the open literature, only a limited number of soot models have been described. Abbas and Lockwood [1985] have developed a simple one step model while a multistep formulation has been developed by Magnussen and Hjertager [1979]. Syed et al [1991] adopted a laminar flamelet approach to computing nonpremixed combustion in which the finite-rate effects were modeled to predict the slow reactions associated with soot formation. In all these approaches, the soot formation process was associated with the local fuel concentration. However, it is well known that the precursor to soot formation is not the parent fuel but pyrolysis products resulting from breakdown of the fuel. In response, Fairweather et al [1992] developed a model of soot formation based on a global reaction scheme in which all the important formation reactions were associated with the pyrolysis products; here taken to be acetylene.

This paper describes the implementation of a variation of the Fairweather et al [1992] soot model in a fully elliptic 3-D body-fitted CFD code based on pressure correction techniques (CONCERT-3D). CONCERT-3D has been used extensively to calculate complex single phase [Shyy et al, 1985; Shyy et al, 1988] and two-phase [Tolpadi,1995] 3-D flow fields in aircraft engine combustors. The code has the capability of analyzing the complex geometrical details of a modern gas turbine combustor, including the swirl cup, splash plate, primary and secondary dilution holes, film cooling slots and multi-hole cooling zones. Initially, the velocity and temperature fields are obtained from CONCERT-3D. Next, the soot predictions were made in post-processing mode by solving two additional transport equations for the soot mass fraction and the soot particle number density. The description of these two equations will be made in the next section.

The soot calculation procedure was first validated against experimental data in a turbulent nonpremixed propane jet diffusion flame in which soot concentration measurements were made by Nishida and Mukohara [1982]. Data were obtained along the centerline, and along the radial direction at five axial stations 100 mm apart beginning from a location 100 mm downstream of the jet. This was done by inserting a soot sampling probe in the flame, collecting the soot over glass wool, and carefully measuring the change in weight of the wool before and after the sampling. The computed soot concentration showed reasonable agreement with the data, certainly the predicted soot levels showed the same trend along the centerline as the data. The level of agreement obtained was found to be about the same as that achieved by Fairweather et al [1992] who used a parabolic code for their computations. As an initial demonstration of this model for combustors, the 3-D flow in three modern aircraft engine combustors (CF6-80LEC, CF6-80C and CFM56-5B) were analyzed over a range of pressures and temperatures. These combustors were studied extensively by Danis et al [1996] and anchored against data. The anchoring process involved calibrating 2−D axisymmetric swirler models against measured values of the swirler exit conditions (velocities, turbulence levels and fuel distribution). The 2−D swirler data was then applied as inlet conditions to the 3−D single cup model using standardized methodology. Even though the fuel in the combustor is Jet−A, for the purpose of the present soot calculations, propane was assumed to be the surrogate fuel. The predicted SAE smoke number based on the computed average combustor exit soot concentration was compared against engine test data.

SOOT MODEL

The soot model is based on a characteristic pyrolysis product, C_2H_2. The soot formation and surface growth reactions are related to the levels of C_2H_2 present in the flame. The oxidation of the soot is caused by O_2, O and OH radicals. The concentration of C_2H_2 and other species were related to the mixture fraction. Prior to performing the soot computations, the distribution of these species is obtained (as a function of the mixture fraction) by running a laminar flamelet (LF) code [Jones and Lindstedt, 1988] from which steady state solutions for a laminar counterflow diffusion flame are obtained along the stagnation point streamline of a porous cylinder. This gives instantaneous relationships between mixture fraction and density, temperature and gaseous composition of the combusting mixture. The strain rate used was 20 sec^{-1}, which is typical of conditions in flames at which most of the sooting is expected to take place [Leung, 1996].

The gas phase flow field is computed by the CONCERT-3D code. The standard k-ε turbulence model is used with wall function treatment for near wall regions. CONCERT-3D is comprised of several combustion models, but the one employed here to obtain the gas temperatures assumes fast chemistry for the gas phase reactions and a shape for the PDF of the mixture fraction. This shape is assumed to be a β-PDF parameterized in terms of the mean and variance of the mixture fraction each of which are modeled by appropriate transport equations [Tolpadi, 1995]. The governing equations of motion are transformed from, in general, an arbitrarily shaped physical domain to a rectangular parallelopiped. The equations are solved in this boundary fitted coordinate system. After making finite difference approximations to the equations, they are solved on a staggered grid by a SIMPLE-like algorithm [Patankar, 1980] extended to the curvilinear coordinate system. The governing equations together with their discretization and the numerical algorithm have been

described in detail in [Tolpadi and Braaten, 1992] and [Shyy and Braaten, 1986].

The computations of soot involve the solution of two additional conservation equations for soot mass fraction and the soot particle number density. The mass fraction equation contains the nucleation (formation), surface growth and oxidation source terms while the number density equation comprises of nucleation and coagulation source terms. Due to the fact that the chemical reactions associated with soot formation are relatively slow, all these source terms can be related to the levels of acetylene and other species which in turn are obtained apriori as a function of the mixture fraction from the LF code. Details of the two equations and source terms are given in [Fairweather et al, 1992] and will only be briefly mentioned here. After performing Favre–averaging of the equations, the source terms of the two transport equations are given by:

$$\rho S(Ycs) = r_i M_{cs} + r_{ii} M_{cs}^{2/3} \rho^{0.5} Ycs^{1/3} N^{1/6} - r_{iii} M_{cs}^{1/3} \rho\, Ycs^{2/3} N^{1/3} \quad (1)$$

$$\rho S(N) = r_{iv} - r_v M_{cs}^{(-1/6)} \rho^2 Ycs^{1/6} N^{11/6} \quad (2)$$

In the above equations, r_i, r_{ii} and r_{iii} are the reaction rate terms representing the formation, surface growth and oxidation of the soot, while r_{iv} and r_v represent formation and coagulation in the number density equation. All these terms are documented elsewhere [Fairweather et al, 1992] but are repeated here for completeness:

$$r_i = C_1 e^{(-21100/T)} [C_2H_2] \quad (3)$$

$$r_{ii} = C_2\, e^{(-12100/T)} A^{0.5} [C_2H_2] \quad (4)$$

$$r_{iii} = C_{33}\, T^{0.5}\, e^{(-19680/T)}\, A\, [O_2] \quad (5)$$

$$r_{iv} = 2N_A\, r_i / C_{min} \quad (6)$$

$$r_v = 2C_a\, (6M_{cs}/\pi\rho_{cs})^{1/6}\, (6kT/\pi\rho_{cs})^{0.5} \quad (7)$$

where $A = \pi(6M_{cs}/\pi\rho_{cs})^{2/3}$

The molar concentrations, which are functions of the temperature and gaseous species concentrations–in turn functions of the mixture fraction–are obtained completely from the laminar flamelet prescription. These terms are convoluted with the beta–PDF that generates apriori a thermochemical table containing the mean reaction rates as a function of the fuel mixture fraction and its variance. In solving the soot equations, the source terms are obtained by 'looking up' this table and performing a bilinear interpolation. As stated earlier, the soot equations can be solved in post–processing mode (or together with the rest of the flow equations). The recommended values of C_1, C_2 and C_{33}, as per [Fairweather et al, 1992] are:

$C_1 = 1.0 \times 10^4$
$C_2 = 1.2 \times 10^4$
$C_{33} = 715$

The oxidation reaction rate requires some discussion. The expression given above and reported by Fairweather et al [1992] was used in the propane jet diffusion flame predictions. However, for the combustor calculations, the oxidation was found to occur very rapidly in the latter half of the combustor (to be described later). With small changes in the oxidation coefficient, very large changes were observed in the predicted smoke number at the combustor exit. In order to improve the sensitivity of the model to the oxidation reaction rate, the contributions of the [O] and [OH] species to soot oxidation were also included in the combustor computations. The assigned collision efficiencies were obtained from the work of Roth and co–workers [1991]. Furthermore, the sensitivity of the local (idealized external) surface area of soot particles was reduced in the manner of Fairweather et al [1992]. Thus, the third term in equation (1) above was modified to:

$$\rho S(Ycs)_{oxidation} = - r_{iii} M_{cs}\, \rho^{0.5}\, Ycs^{1/3}\, N^{1/6} \quad (8)$$

$$\text{where, } r_{iii} = (\pi T)^{0.5} (6/\pi\rho_{cs})^{1/3} \left(C_3(0.441[OH] + 1.818[O]) + C_4 * 4.649 e^{(-11250/T)} [O_2] \right) \quad (9)$$

Here C_3 and C_4 are coefficients that independently control the level of oxidation caused by the ([O]+[OH]) radicals and by $[O_2]$ respectively. Recommended values are:

$C_3 = 1.0$
$C_4 = 1.0$

There will be more discussions on these coefficients that will appear later.

RESULTS

The soot model was initially validated against propane jet diffusion flame data [Nishida and Mukohara, 1982] taken at atmospheric pressure. In this flame, propane issued from a 2 mm diameter pipe at 30 m/s and burnt with stabilization being provided by a pilot flame. This pipe was placed in an annulus of diameter 105 mm and 1 meter length. Air entered the annulus at two average inlet velocities of 0.40 and 0.96 m/s corresponding to the preheat temperatures of 323 and 773 deg K that were studied. The computed soot concentration profiles were compared with the data. Even though this geometry is 2–D axisymmetric, it was modeled in this study as a 3–D object by generating a polar grid with a 15 degree sector angle. This was done keeping in mind the fact that the ultimate objective was to perform 3–D combustor computations. The grid used for this calculation extended the entire length of the annulus. In the radial direction, the grid was fine near the fuel jet. There were 250 cells in the axial and 30 cells in the radial direction. The solution of this 2–D problem using the 3–D CONCERT code required that at least 3 cells be placed in the angular direction. Calculations for this problem were carried out on an HP–735 workstation. In the computations of this flame presented in [Fairweather et al, 1992], the authors state that the flamelet temperatures required an adjustment to account for the radiative heat loss. This adjustment derived from adiabatic laminar calculations was

made by matching the turbulent flame predictions with the peak mean temperature measured within the flames. Accordingly, the temperatures were scaled down (with appropriate scaling of the density) using the same technique. The resulting lower temperature (as opposed to equilibrium temperatures) as a function of the mixture fraction was used to generate the thermochemical tables for the soot computations.

Fig. 1 shows the soot concentration along the centerline for the 323 deg K preheat temperature case. The predicted soot concentration increases rapidly in the initial regions of the flow before oxidizing and burning out. The location of the predicted peak is about the same as the corresponding data, but its magnitude appears to be underpredicted. Fig. 2 shows the radial profiles of the soot concentration at five axial locations from 0.1 to 0.5 m. This figure also indicates that the soot levels initially increase upto x=0.3m before they start decreasing. The magnitudes of the soot concentration at the different axial stations appear to be underpredicted by about a half order of magnitude. The oxidation of the soot beyond the peak location also appears to be taking place faster than that suggested by the data. The level of agreement with the data obtained by Fairweather et al [1992] with a parabolic code is about the same as that indicated in these two figures.

Figs. 3 and 4 show the same predictions for the 773 deg K preheat temperature case. Once again the soot levels have been underpredicted by about a half order of magnitude and the oxidation is predicted to take place faster than that observed experimentally. Comparison of Fig. 3 with Fig. 1 indicates that the effects of higher preheat temperature are (1) to generate higher peak levels of the soot and (2) to shift the location of the peak further upstream. Figs. 1–4 clearly indicate the fact that the model is doing well in calculating the production of the soot but predicts its burn out to take place too rapidly. This suggests that improvements have to be made in predicting the accuracy of O_2 levels within the flame, and that also the effects of O and OH radicals on the oxidation should be included. This is the motivation behind the modifications made to the oxidation term described in the previous section. Calculations of this propane flame with the modified oxidation expression (equation (8)) were not actually performed, but were used only for the combustor computations to follow. In addition, intrinsic difficulties associated with the presumed β–PDF approach and turbulent transport are also likely to play a significant role.

Fig. 5 shows a schematic of one of the aircraft engine combustors studied–the CF6–80C. It is of single annular design with 30 swirl cups equally spaced around the circumference. Within a single–cup section, there are 10 dilution holes (6 top and 4 bottom) and 14 film cooling slots (7 top and 7 bottom) along the liner walls. To model the entire combustor, only one section is considered with periodic boundary conditions imposed on the side planes [Tolpadi, 1995]. The mesh generated to model this combustor had a total of 63423 grid points (58240 computational cells). The results to follow are divided into two parts: the first study focuses on a specific temperature and pressure at which the effect of the soot model parameters on the prediction is examined while in the second study, the effect of the combustor operating conditions (pressure and temperature) on the soot prediction is considered.

Fig. 6 shows the temperature distribution in a side view through the middle of the swirl cup of the CF6–80C combustor calculated at high power conditions (30 atm. and 860 deg K at combustor inlet). No data exists that would validate the temperature field predicted in the interior of the combustor, but the anchoring process involves matching the predicted exit temperatures with the corresponding rig data [Danis et al, 1996; Tolpadi, 1995; Shyy et al, 1988]. Having obtained this temperature distribution with CONCERT–3D, the soot calculations were performed in postprocessing mode. One of the first consequences of assuming propane to be the surrogate fuel for soot calculations in the combustor burning Jet–A fuel is that the production of the soot would be underpredicted. This is because Jet–A fuel contains many aromatic soot precursors whereas propane fuel in this model has acetylene as the only soot precursor. Work is currently underway to incorporate a kerosene model that would account for other precursors, however in the interim the production coefficient in this first study was increased by a factor of 10 to $C_1=1\times10^5$. Fig. 7 shows the soot mass fraction contours in a side view in the same plane as Fig. 6. Significant amount of soot is produced in the primary zone of the combustor which quickly oxidizes in the latter half of the combustor. The soot measurements made at the exit of the engine were reported in terms of the SAE smoke number. The relationship between the smoke number and average exit soot concentration, C_{av}, (kg/m**3) is as follows [Champagne, 1971]:

$$\text{SAE \#} = 4.641\times10^{16}C_{av}^3 - 1.200\times10^{12}C_{av}^2 + 1.188\times10^{7}C_{av} \qquad (10)$$

This relationship is valid upto an SAE # of 100. At the conditions of Fig. 6, the measured smoke number at the exit was 17.0. This corresponded to a concentration of about 1.6×10^{-6} kg/m**3 or a mass averaged exit mass fraction of 2.6×10^{-7}. This soot mass fraction is over 5 orders of magnitude smaller than the peak soot mass fraction in the primary zone in Fig. 7. The reason for emphasizing these quantities is to give an idea of the magnitude of the problem that is being studied here. Even though the levels of peak soot in the combustor may be reasonably well predicted, it is the tail end of the oxidation that has to be resolved in the combustor and this was found to be quite a monumental task. The computed SAE smoke number was found to be quite sensitive to the specified oxidation coefficients C_3 and C_4. Since O_2 is the primary specie responsible for oxidation, the coefficient C_3 was set to its recommended value of unity, but the coefficient C_4 was allowed to vary (Note that the recommended value of C_4 is also unity). The uncertainties associated with the collision frequency assumed for the oxidation rate justifies the use of an increased oxidation coefficient. Fig. 8 shows the computed smoke number as a function of the O_2 oxidation coefficient. The predicted smoke number decreases as the coefficient, C_4, increases. Actually, the original oxidation model (with r_{iii} given by equation (5)) was initially employed but the predicted smoke number was found to be even more sensitive to the oxidation coefficient C_{33} (Fig. 9). Consequently, the modified oxidation model was used in all combustor computations.

In the second study, a CF6–80LEC combustor was run at four operating conditions ranging from 45% to 100% power. The smoke numbers measured during certification testing at these conditions range from 0.0 to 6.8 as seen in Table 1. The corresponding measured soot concentrations are also shown. The predicted soot concentrations at the combustor exit for these four power conditions are also shown

in Table 1, for the soot model run under four different modes: 1) with nominal production and oxidation coefficients, 2) with 4X oxidation coefficient, 3) with 10X production coefficient and 4) with 4X oxidation and 10X production coefficients. The nominal production coefficient corresponds to the constant $C_1=1.0\times10^4$, and the nominal oxidation coefficient corresponds to $C_3=C_4=1.0$. By 4X oxidation, it is meant that $C_3=1.0$ and $C_4=4.0$. Likewise, 10X production means that $C_1=1.0\times10^5$. The results clearly show that the basic model overpredicts soot concentration by 2–4 orders of magnitude over the power range. The agreement is much closer when the oxidation coefficient is increased by a factor of four, but does not agree over the entire power range. The other two cases with increased soot production, 10X, both overpredict soot concentration. Table 1 also summarizes the calculations with models of a CF6–80C and a CFM56–5B run at full power. (It should be noted that the CF6–80C combustor result shown in this table is not the same as that described in the first study. This is because the combustor in this table has an improved swirl cup design resulting in less smoke.) The results obtained are very similar to the CF6–80LEC results wherin increase of the oxidation coefficient by 4X brought the predicted soot concentration closer in order of magnitude to the measurements. These calculations again demonstrate that the soot model is very sensitive to changes in the oxidation parameter. The oxidation terms could be tuned to match individual power points for a given combustor, but that would not result in a useful design tool. There are several issues with regard to making improvements in the modeling approach which will be discussed in the next section.

CONCLUSIONS AND FUTURE DIRECTIONS

A simplified soot formation, growth and consumption model has been incorporated into a three–dimensional body–fitted CFD code (CONCERT–3D) for the prediction of soot in gas turbine combustors. The gas temperature field is obtained via a prescribed PDF approach assuming fast chemistry. The soot levels are then predicted through the solution of transport equations for the soot mass fraction and the soot particle number density which both admit finite–rate kinetics. These equations contain source terms that represent the production, surface growth and oxidation of the soot that are related to certain species whose distributions are obtained apriori from a laminar flamelet code. To initially validate the model, calculations of the soot concentration were performed in a simple propane jet diffusion flame in which data were obtained by Nishida and Mukohara [1982]. The comparison obtained was reasonable, but the soot levels were underpredicted and the soot oxidation was found to proceed more rapidly.

Calculations of sooting levels were next performed in three different aircraft engine combustors. Propane was assumed to be the surrogate fuel in these calculations. It was not possible to obtain a single set of model constants applicable universally to all combustors. In fact, it was not possible to obtain a single set of production and oxidation coefficients that would make reliable soot predictions over the entire operating range of a specific combustor. The choice of propane as the surrogate fuel and aceylene as the precursor to soot formation is expected to underpredict the actual soot production. A kerosene model that employs benzene and other aromatic compounds as precursors to soot formation is currently being developed to improve modeling of the soot production. However, the oxidation of the soot was found to be the most difficult aspect to model. The predicted exit soot concentration was found to be quite sensitive to the oxidation coefficient. More work needs to be done to establish the role of gas phase activation of soot particle sites that would be based on a similarity with the oxidation of aromatic molecules. Indications are that soot oxidation by molecular oxygen requires activation of the soot surface by radical species. In addition, the present soot model makes an important assumption of a single particle size at every location–this means that the soot particle size can vary within the combustor but at a specific location, a single size alone is assumed to contribute to the computed soot mass fraction. This is obviously not true and is an assumption that has been made here to simplify the model. The procedure to model variable particle size is to first define a series of bins–each bin over a certain particle size range. Transport equations have to be written for each bin with the overall soot concentration at any location defined to be the sum total of the contributions from each bin. Turbulence modeling is also an important issue in soot modeling. In the present approach, turbulent transport of particles is modeled via the standard k–ε model. It is well known that the k–ε model does not accurately predict mixing in strongly recirculating flows such as those present in gas turbine combustors. The Reynolds Stress Turbulence Model (RSTM) of Launder [1995] is currently being pursued. Finally, it is well known that the prediction of soot by any model greatly depends on the temperature field. As stated earlier, only the exit combustor temperatures predicted were matched with aircraft engine data. Since soot is produced in the primary zone, it is necessary to also validate by some means the predicted interior combustor temperatures as well.

REFERENCES

[1] Abbas, A.S., and Lockwood, F.C., 1985, *J Inst. Energy*, Vol. 58, pp. 112.

[2] Champagne, D.L., 1971, "Standard Measurement of Aircraft Gas Turbine Engine Exhaust Smoke", ASME Paper 71–GT–88.

[3] Danis, A.M., Burrus, D.L., and Mongia, H.C., 1996, "Anchored CCD for Gas Turbine Combustor Design and Data Correlation", ASME Paper 96–GT–143, Accepted for publication *ASME J. Engg. for GT & Power.*

[4] Fairweather, M., Jones, W.P., Ledin, H.S., and Lindstedt, R.P., 1992, "Predictions of Soot Formation in Turbulent Non–Premixed Propane Flames", *Proc. of 24th Int. Symp. on Combustion*, pp. 1067–1074.

[5] Jones, W.P., and Lindstedt, R.P., 1988, "The Calculation of the Structure of Counterflow Diffusion Flames using a Global Reaction Mechanism", *Comb. Sci. and Tech.*, Vol. 61, pp. 31–49.

[6] Launder, B.E., 1995, "Modelling the Formation and Dispersal of Streamwise Vortices in Turbulent Flow", *Aero. J. of the Royal Aero. Soc.*, Vol. 99, pp. 419–431.

[7] Leung, K.M., 1996, "Kinetic Modelling of Hydrocarbon Flames using Detailed and Systematically Reduced Chemistry", Ph.D. Thesis, University of London.

[8] Magnussen, B.F., Hjertager, B.H., Olsen, J.G., and Bhaduri, D., 1979, "Effects of Turbulent Structure and Local Concentration on Soot Formation and Combustion in Acetylene Diffusion Flames", *Proc. of 17th Int. Symp. on Combustion*, pp. 1383–1393.

[9] Nishida, O., and Mukohara, S., 1982, "Characteristics of Soot Formation and Decomposition in Turbulent Diffusion Flames", *Combustion & Flame*, Vol. 47, pp. 269–279.

[10] Patankar, S.V., 1980, *Numerical Heat Transfer and Fluid Flow*, McGraw Hill Hemisphere, New York.

[11] Roth, P., Brandt, O., and Von Gersum, S., 1990, "High Temperature Oxidation of Suspended Soot Particles Verified by CO and CO_2 Measurements", *Proc. of 23rd Int. Symp. on Combustion*, pp. 1485–1491.

[12] Shyy, W., and Braaten, M.E., 1986, "Three–Dimensional Analysis of the Flow in a Curved Hydraulic Turbine Draft Tube", *Intl. J. Numer. Meths. Fluids*, Vol. 6, pp. 861–882.

[13] Shyy, W., Correa, S.M., and Braaten, M.E., 1988, "Computation of Flow in a Gas Turbine Combustor", *Combust. Sci. and Tech.*, Vol. 58, pp. 97–117.

[14] Shyy, W., Tong, S.S., and Correa, S.M., 1985, "Numerical Recirculating Flow Calculations Using a Body–Fitted Corrdinate System", *Numer. Heat Trans.*, Vol. 8, pp. 99–113.

[15] Syed, K.J., Stewart, C.D., and Moss, J.B., 1990, "Modeling Soot Formation and Thermal Radiation in Buoyant Turbulent Diffusion Flames", *Proc. of 23rd Int. Symp. on Combustion*, pp. 1533–1541.

[16] Tolpadi, A.K., 1995, "Calculation of Two–Phase Flow in Gas Turbine Combustors", *ASME J. Engg. for Gas Turbines and Power*, Vol. 117, pp. 695–703.

[17] Tolpadi, A.K., and Braaten, M.E., 1992, "Study of Branched Turboprop Inlet Ducts Using a Multiple Block Grid Calculation Procedure", *ASME J. Fluids Engg.*, Vol. 114, pp. 379–385.

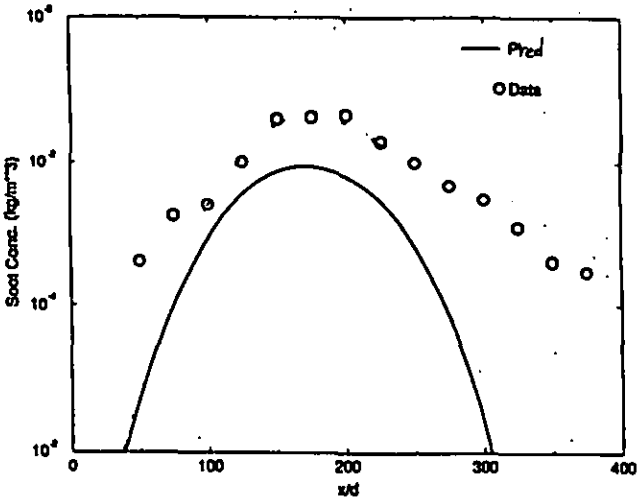

Fig. 1. Predicted and measured [Nishida and Mukohara, 1982] soot concentration along the centerline of propane jet diffusion flame with 323 deg K preheat temperature

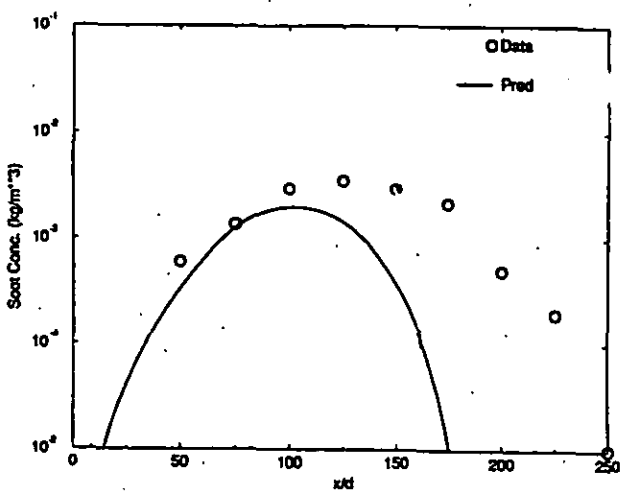

Fig. 3. Predicted and measured soot concentration along the centerline of propane jet diffusion flame with 773 deg K preheat temperature

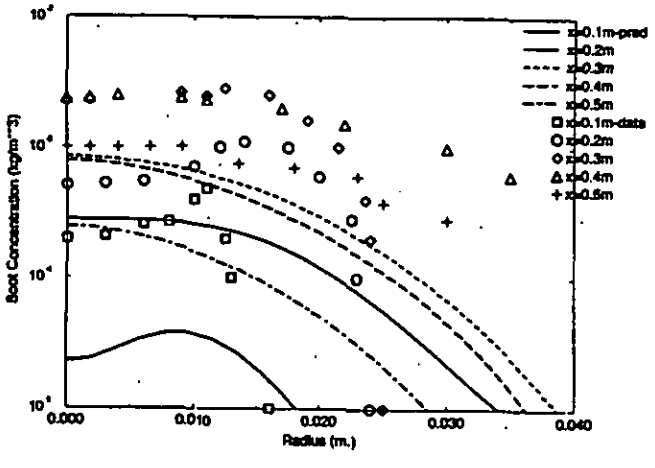

Fig. 2. Predicted and measured radial soot concentration at different axial locations of propane jet diffusion flame with 323 deg K preheat temperature

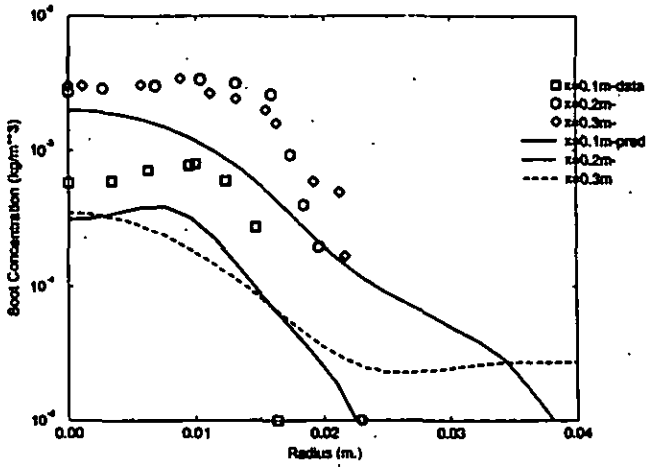

Fig. 4. Predicted and measured radial soot concentration at different axial locations of propane jet diffusion flame with 773 deg K preheat temperature

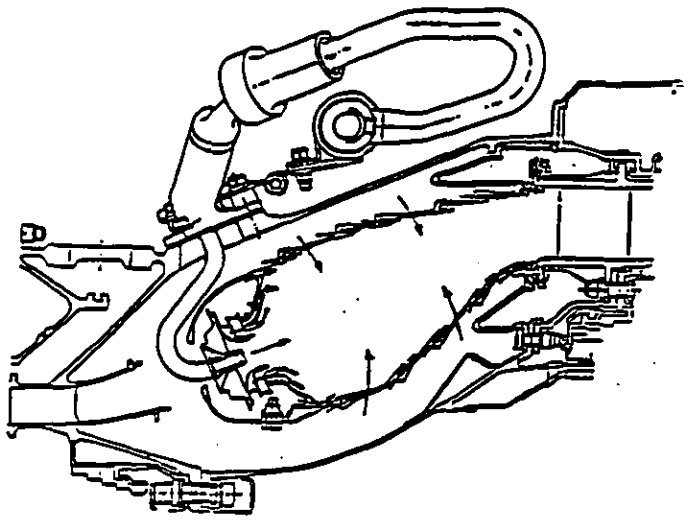

Fig. 5. Geometry of a CF6–80C low emissions single annular aircraft engine combustor

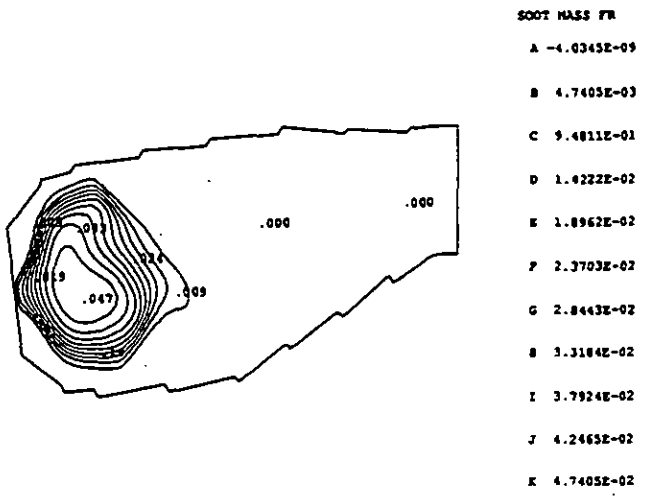

Fig. 7. Calculated soot mass fraction contours in a side view through the swirl cup of the CF6–80C combustor, P3=30 atm., T3=860 deg K

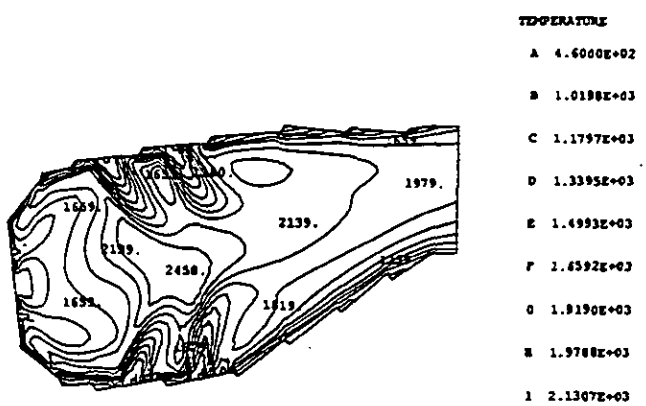

Fig. 6. Calculated temperature contours (deg K) in a side view through the swirl cup of the CF6–80C combustor, P3=30 atm., T3=860 deg K

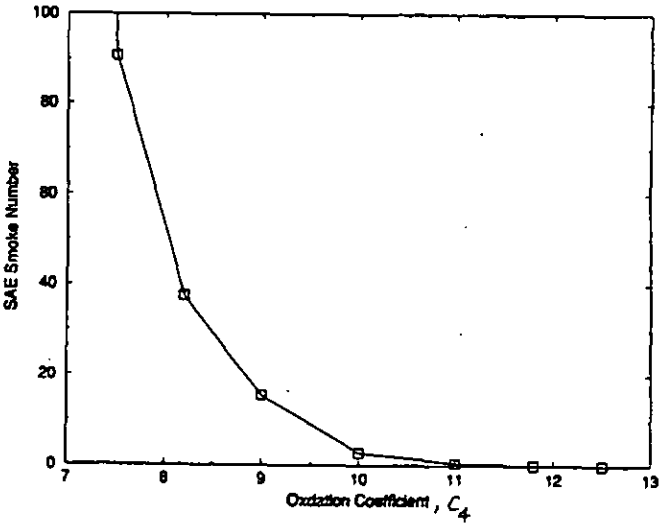

Fig. 8. Effect of oxidation coefficient on the predicted smoke number of CF6–80C combustor (modified oxidation model), P3=30 atm., T3= 860 deg K, C_3=1.0

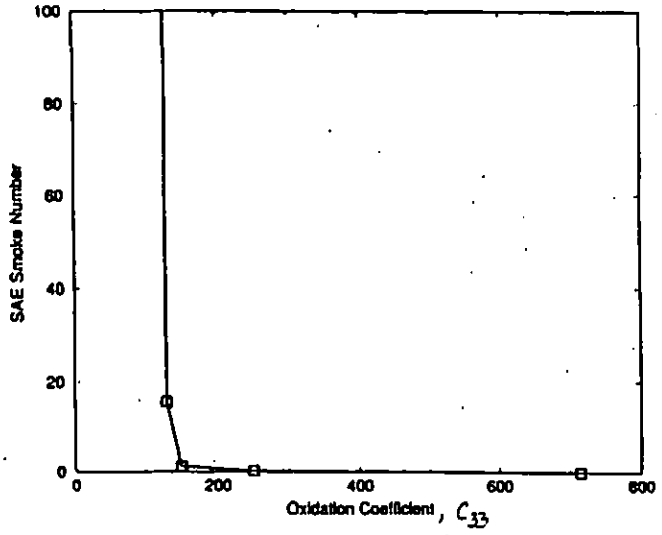

Fig. 9. Effect of oxidation coefficient on the predicted smoke number of CF6–80C combustor (original oxidation model as per Fairweather et al [1992]), P3=30 atm.; T3=860 deg K

COMBUSTOR ENGINE MODEL	POWER RATING (%)	MEAS. SMOKE NUMBER	MEAS. SOOT CONC. (kg/m^3)	PRED. SOOT CONC. (kg/m^3)	PRED. SOOT CONC. (kg/m^3)	PRED. SOOT CONC. (kg/m^3)	PRED. SOOT CONC. (kg/m^3)
OXIDATION COEFFICIENT:				1X	4X	1X	4X
PRODUCTION COEFFICIENT:				1X	1X	10X	10X
CF6-80LEC	100	6.8	7.19E-07	1.62E-03	1.38E-05	2.68E-03	3.15E-05
CF6-80LEC	85	5.9	6.57E-07	3.24E-04	4.12E-07	7.25E-04	1.86E-06
CF6-80LEC	70	2.7	2.00E-07	2.91E-05	5.50E-13	8.10E-05	4.23E-11
CF6-80LEC	45	0	0.00E+00	8.80E-13	3.00E-13	3.14E-05	1.43E-12
CF6-80C	100	8.8	8.62E-07	1.28E-03	1.55E-05	2.12E-03	4.78E-05
CFM56-5B	100	8.0	8.12E-07	1.69E-03	5.88E-05	2.54E-03	1.18E-04

Table 1. Measured and predicted soot concentrations (kg/m**3) for three combustors at different operating conditions